Analysis of Crack Resistance of Asphalt Concrete Overlays—A Fracture Mechanics Approach

YEOU-SHANG JENQ, CHWEN-JANG LIAW, AND PEI LIU

Cracking is one of the major distress modes that cause premature failure of asphalt concrete pavements. Formation of cracks in asphalt concrete pavements can be the result of the following: applied traffic loads, temperature-induced thermal stresses, freeze-thaw damage due to water infiltration, aging effects, and so forth. A conceptual framework to characterize (and quantify, if possible) the crack resistance of asphalt concrete pavement systems based on a fracture mechanics theory is presented. A cohesive crack model, which is similar to the Dugdale-Barenblatt type of models proposed for ductile yielding of metals, was used to simulate the progressive crack formation and propagation in asphalt concrete. A parametric study was conducted to study the effects of temperature, fiber reinforcement, and overlay thickness on the crack resistance of asphalt concrete overlays. It was found that a thicker overlay has a much higher temperature crack resistance, which is in agreement with general field observations. Furthermore, although it was found that at lower service temperature the overlay has a much higher temperature resistance, this improvement is not enough to compensate for a much larger temperature differential and contraction displacement caused by the service temperature drop. Fiber reinforcement was found to slightly increase the crack resistance of the asphalt concrete overlays. It was further observed that the temperature crack resistance is proportional to the increase of the tensile strength.

Cracking is one of the major distress modes that cause premature failure of asphalt concrete pavements. Formation of cracks in asphalt concrete pavements can be the result of the following: applied traffic loads, temperature-induced thermal stresses, freeze-thaw damage due to water infiltration, aging effects, and so forth. Because of the complexity involved in the development of cracks in asphalt concrete, there is currently no unique approach accepted by researchers to characterize the crack resistance of asphalt concrete pavement systems. The present paper is an attempt to present a conceptual framework initially to characterize (and quantify, if possible) the crack resistance of asphalt concrete pavement systems based on fracture mechanics theory.

A cohesive crack model, which is similar to the Dugdale-Barenblatt type of models proposed for ductile yielding for metals, is used in the present study to simulate the progressive crack formation and propagation in asphalt concrete. A parametric study of the effects of temperature on the crack resistance of asphalt concrete overlays was performed to demonstrate the feasibility of the proposed approach in characterizing the fracture response of flexible pavement systems. The theoretical results were found to be in agreement with commonly reported field observations, which indicates that the proposed fracture mechanics approach has its potential in analyzing asphalt concrete pavement systems subjected to more complex service conditions. In addition, it is believed that the material properties associated with the proposed fracture mechanics model can be used as criteria in designing good-quality asphalt concrete mixes with better crack resistance.

Department of Civil Engineering, The Ohio State University, Columbus, Ohio 43210.

PROPOSED COHESIVE CRACK MODEL

In modeling crack formation and crack propagation, the crack can generally be modeled as the Griffith type of traction-free cracks or the Dugdale-Barenblatt type of cohesive cracks. It is believed that the cohesive type of cracks is more suitable in describing the nature of cracks in viscous materials such as asphalt concrete. The cohesive crack concept assumes that when a crack starts to develop in a material, the crack is still able to transfer some forces. The crack zone that is bridged by this cohesive force, which is generally termed the "process zone," is governed by the applied load, structure/sample geometries, and the basic properties of the material. The cohesive crack concept was originally proposed by Dugdale (*1*) and Barenblatt (*2*) for metals and by Hillerborg et al. (*3*) for portland cement concrete to characterize progressive crack development in the materials.

To simulate crack formation and propagation in asphalt concrete, a cohesive crack model that is similar to the Dugdale-Barenblatt cohesive crack model discussed earlier was proposed by Jenq and Perng (*4*). Because of the viscous nature of asphalt concrete, the cohesive stress was assumed to be time dependent and temperature dependent, and may be modeled using various combinations of nonlinear springs and dashpots (see Figure 1). In addition, several assumptions were proposed in the proposed model:

1. The process zone is assumed to initiate at the point when the first principal stress reaches the tensile strength (f_t; see Figure 2*a* and *b*).
2. The direction of the process zone will be perpendicular to the direction of the first principal stress.
3. The properties of the materials outside the process zone are governed by a stress-strain relationship (Figure 2*a*), which is dependent on the applied loading rate and service temperature.

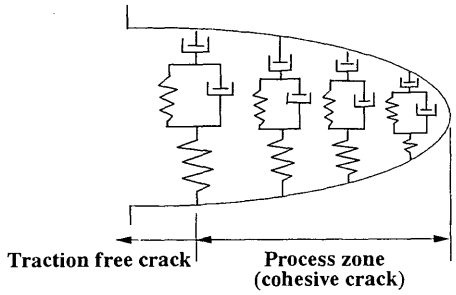

FIGURE 1 Cohesive crack modeled using nonlinear springs and dashpots.

4. The material in the process zone is able to transfer stress, and the stress-transferring capability depends on its opening according to the stress-separation relationship shown in Figure 2*b*. This stress-separation relationship is a function of loading rate and temperature. The area under the stress-separation curve is defined as fracture energy (G_f), which represents the energy needed to create a unit of traction-free surface.

On the basis of these assumptions, the size of the process zone, the magnitude of the bridging stress, and the applied load can be determined accordingly (*4*,*5*). The proposed stress-separation curve concept is the key factor that separates the proposed fracture mechanics model from conventional strain-based or stress-based models. Since strain cannot be objectively defined when there is displacement discontinuity (e.g., a crack), a fracture mechanics model will be more suitable in characterizing fracture mechanisms in a material.

NUMERICAL FORMULATION

For simplicity, a notched beam is used to demonstrate the numerical formulation for the proposed cohesive crack model. Consider a notched beam with a preexisting crack up to Node n subjected to a load P in the midspan, as shown in Figure 3*a*. It is assumed that the process zone will develop along a straight plane, which is reasonable for Mode I crack propagation. When the beam is loaded, by introducing the closing stresses over the crack, one can analyze the progressive crack development in the beam (*5*).

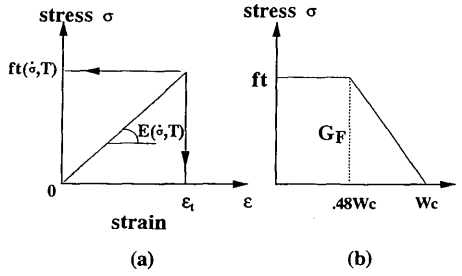

FIGURE 2 (*a*) Stress-strain curve for asphalt concrete before process zone initiation and (*b*) proposed σ-*w* curve for asphalt concrete after process zone initiation.

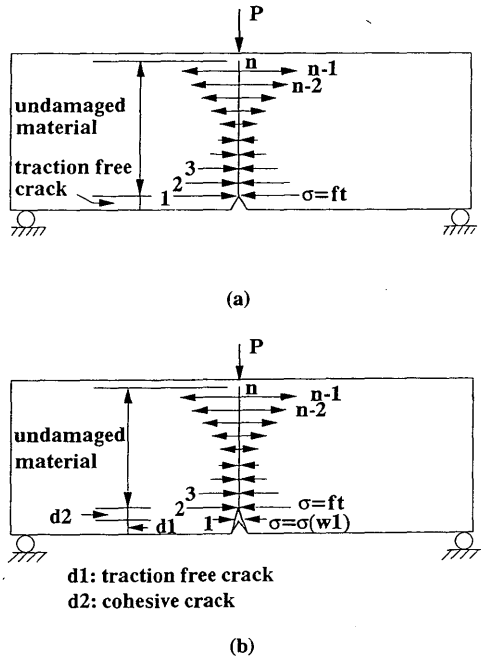

FIGURE 3 (*a*) Notched beam subjected to three-point bending and (*b*) crack propagation to the second point.

In the calculation process, the stresses acting across the cohesive crack were replaced by equivalent nodal forces. These forces can be determined according to the stress-separation curve when the width at the cohesive crack zone is known. As indicated in Figure 3*a*, when the first node reaches its tensile strength, the opening displacement at the first node is still equal to zero, that is, $\sigma_1 = f_t$, $w_1 = \ldots = w_{n-1} = 0$. From this, one can determine the first point, which corresponds to the crack initiation point, of the load-load line deflection ($P - \delta$) curve and the load-crack mouth opening displacement (P-CMOD) curve.

When the crack starts to propagate, as shown in Figure 3*b*, the first node is opened and the second node is assumed to reach the tensile strength. At this point the boundary conditions can be expressed as $\sigma_2 = f_t$, $w_2 = w_3 = \ldots = w_{n-1} = 0$, $w_1 \neq 0$, and $\sigma_1 = \sigma(w_1)$. The system equations are nonlinear because of the stress-separation constraint. Therefore, an iteration process is needed for this step.

Following the same principle, the progress of crack propagation can be analyzed, and complete $P - \delta$ and P-CMOD curves can be generated. On the basis of the proposed cohesive crack model, no tensile stress will be transferred along the crack surfaces when the crack opening displacement is larger than the critical crack opening displacement (w_c), which is equal to $G_f/(0.74f_t)$ for the proposed stress-separation curve, as indicated in Figure 2*a*. The critical crack opening displacement is about 0.102 and 0.178 cm at 0°C for plain asphalt concrete and fiber-reinforced asphalt concrete, respectively. More detailed numerical formulation was given previously (*4*,*5*). The driving force for crack propagation in a pavement system is not limited to the applied load (P). Service temperature differential (T), which is defined as the temperature difference from the surface to a certain depth of the pavement,

can also be the driving force for crack propagation. The principle involved in the numerical formulation, however, is the same for the applied load and service temperature. Thus, one can derive the numerical formulation for temperature loading by replacing the effect of applied load with that of temperature. To obtain the theoretical results using the proposed cohesive crack model, a numerical method such as the finite element method has to be applied.

NUMERICAL EXAMPLE

To demonstrate the applicability of the proposed cohesive crack model, a parametric study on the reflective crack resistance of asphalt concrete overlays to temperature differentials was performed. The reflective cracking in asphalt concrete overlays is mainly the result of the contraction and curling actions of the overlaid old pavements caused by temperature differentials and the applied traffic loads. For the present analysis, only temperature effect is considered, and the pavement system is simulated using a two-dimensional model. Furthermore, only the effect of a single temperature cycle is analyzed in the present study. A complete analysis, of course, should include the effect of temperature cycles (*6*), which is currently under way and will be reported elsewhere. Although temperature-induced reflective cracking can be modeled as a Mode I crack, mixed mode failure conditions may occur under the application of traffic load, which will generate a much higher compressive stress and shear stress in the overlay.

The pavement system analyzed was a three-layer system in which there is an asphalt concrete overlay over existing concrete slabs. The thicknesses for the concrete slabs and subgrade soil were 22.86 and 203.2 cm, respectively. Three different overlay thicknesses (i.e., 5.08, 10.16, and 15.24 cm) were analyzed. The length of the jointed slabs is 731.52 cm. Material properties such as Young's modulus, coefficient of thermal expansion, and Poisson's ratios for each layer were listed in Figure 4 along with the prescribed boundary condition. Because of the symmetry condition of the pavement, only half of the slab was analyzed. No initial crack or notch was imposed on the asphalt concrete overlay. The existence of the concrete joint, which creates a very high stress concentration at the joint-overlay interface, was simulated as an existing crack. Thus, the reflective crack was assumed to initiate from the bottom of the overlay and propagate upwards.

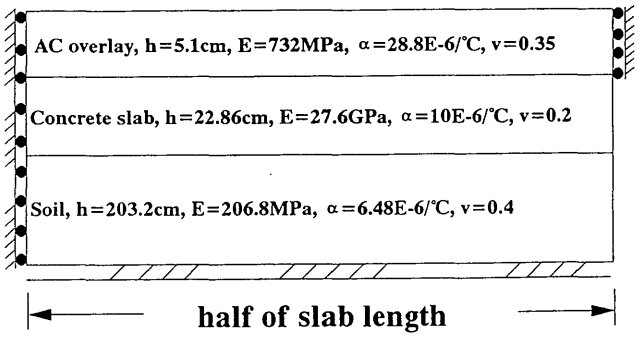

FIGURE 4 Boundary conditions.

Because temperature is the driving force in the present study, temperature distribution in the pavement has to be prescribed first. A parabolic equation was used to describe the temperature distribution along the depth of the pavement. This assumption was based on the results of field temperature measurement (see Figure 5) (*7,8*). It was further assumed that the temperature differential below 38.1 cm of the pavement surface is zero. A typical unit temperature differential profile is given in Figure 6. Because the material properties such as the fracture energy, modulus of elasticity, and fracture energy values are also dependent on service temperature, for simplicity, material properties associated with the model were also assumed to be the same as those measured at a constant service temperature throughout the analysis. When the temperature profile is known, the effects of temperature differential (T) on the crack resistance of the pavement system can be performed.

Based on the same numerical formulation principle discussed earlier, the opening displacement of the crack at each node and at the reference point can be calculated from the following equations:

$$w_i = \sum_{j=1}^{n-1} a_{ij}\sigma_j + c_j T \tag{1}$$

$$w_R = \sum_{j=1}^{n-1} b_j\sigma_j + d_T T \tag{2}$$

$$\begin{bmatrix} a_{11} & a_{12} & \cdots & a_{1(n-1)} & c_1 \\ a_{21} & a_{22} & \cdots & a_{2(n-1)} & c_2 \\ \cdots & \cdots & \cdots & \cdots & \cdots \\ a_{(n-1)1} & a_{(n-1)2} & \cdots & a_{(n-1)(n-1)} & c_{n-1} \\ b_1 & b_2 & \cdots & b_{n-1} & d_T \end{bmatrix} \begin{bmatrix} \sigma_1 \\ \sigma_2 \\ \vdots \\ \sigma_{n-1} \\ T \end{bmatrix} = \begin{bmatrix} w_1 \\ w_2 \\ \vdots \\ w_{n-1} \\ w_R \end{bmatrix} \tag{3}$$

or

$$\{C\}[F] = [\Delta] \tag{4}$$

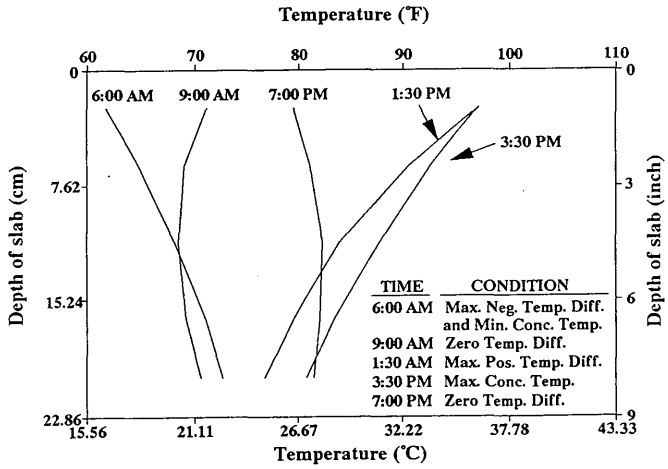

FIGURE 5 Typical temperature gradient for a 22.86-cm slab (*7*).

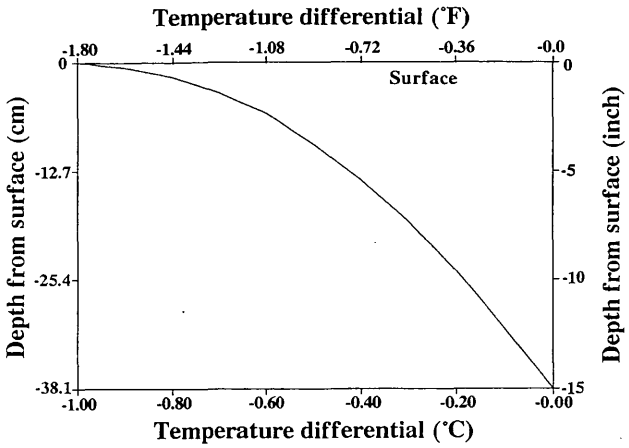

FIGURE 6 Temperature profile used in the present study.

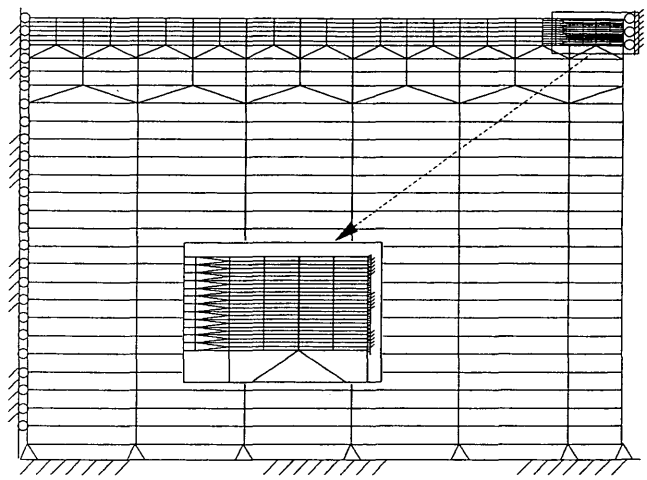

FIGURE 7 Finite element mesh used in the influence matrix generation.

where

a_{ij} = the opening displacement of the crack at Node i when an equivalent closing force is acting at Node j,
c_j = the opening displacement of the crack at Node i when a unit-negative temperature differential is applied,
b_j = the displacement at the reference point when an equivalent closing force is acting at Node j,
d_T = the opening displacement at the reference point when a unit-negative temperature differential is applied,
σ_j = the closing pressure at Node j, and
w_R = the displacement at the reference point.

The square matrix, $\{C\}$, in Equation 4 is referred to as the influence matrix. In the influence matrix, except for the last column, the ith column represents the opening displacement at each node and at the reference point when a pair of equivalent unit closing forces acts at the ith node point. The last column represents the openings at each node and the displacement at the reference point when a negative unit temperature differential is applied. ABAQUS finite element package was used to generate the influence matrix, and the finite element mesh used in the analysis is given in Figure 7. The vector $[F]$ represents the closing pressure at each node and the applied temperature differential, and the vector $[\Delta]$ represents the opening displacement at each node and the reference point.

Thus, based on the calculation procedures discussed earlier, a complete temperature differential versus CMOD curve and crack growth development as a result of temperature differential can be generated. The definition of CMOD used here is the same as the joint opening displacement of the concrete slabs (Figure 8).

MATERIAL CHARACTERIZATION

To perform the analysis, proper material properties such as Young's modulus (E), shape of the stress-separation curve, fracture energy (G_f), and the tensile strength (f_t) associated with the proposed model have to be evaluated first. The stress-separation relationship reported by Jenq and Perng (*4*), as shown in Figure 2, was used in the present study. For the post-crack stress-separation relationship, a ductile Dugdale type of bridging stress is first encountered and then the bridging stress decreases as the separation increases. When the crack opening is larger than the critical crack opening displacement (w_c), the bridging stress diminishes. The fracture energy, which has the same value as the area under the stress-separation curve, was determined from a notched half-disk fracture mechanics test, and the tensile strength was obtained from the indirect tensile tests (*4,9*). Values of E, G_f, and f_t at different temperatures reported by Jenq and Liu (*9*) were used as the material properties for asphalt concrete overlays. The modulus of elasticity determined using the indirect tensile test, which was used in the present study, is much lower than those determined from the resilient modulus test because of the very low loading rate used in the indirect tensile tests (*9*). The mix proportions and the associated material properties of plain asphalt concrete and fiber-reinforced asphalt concrete are listed in Tables 1 and 2, respectively. Detailed material properties and testing methods used to determine these values were given previously (*9*).

In addition to the above-mentioned material properties, to perform the analysis one also has to know the coefficient of thermal expansion, the Poisson's ratios, and the modulus of elasticity of the base material and the soil. For the present

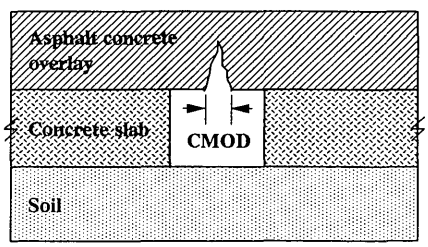

FIGURE 8 Crack mouth opening displacement (CMOD) in the concrete pavement system.

TABLE 1 Mixing Parameters for Various Series of Asphalt Concrete

Series	Fiber type	Fiber weight content (%)	Fiber volume fraction (%)	Asphalt content (%)	Mixing temperature (°C)
A	***	0	0	5.5	152
F	polyester	0.3045	0.593	5.8	152
G	polypropyl-ene	0.2724	0.688	5.8	146

TABLE 2 Material Properties of Various Series of Asphalt Concrete

	Temperature	A[a]	F[a]	G[a]
Young's Modulus E (MPa)[b]	0°C	732.2	784.6	805.3
	23°C	219.7	211.0	196.7
Fracture Energy Gf (N/m)[c]	0°C	5248.3	7815.5	8430.9
	23°C	1270.5	2089.2	1705.7
Tensile Strength ft (MPa)	0°C	1.130	1.235	1.282
	23°C	0.278	0.361	0.325
Poisson's Ratio	0°C	0.25	0.25	0.25
	23°C	0.35	0.35	0.35
Coefficient of thermal expansion ($*10^{-6}$/°C)	***	28.8	28.8	28.8

[a] Related mix information of series A, F, and G is given in Table 1.
[b] 1 Pa = 0.000145 psi.
[c] 1 N/m = 0.00571 lbs/in.

analysis, typical values reported by various researchers on these materials were used and given in Figure 4.

PARAMETRIC STUDY

On the basis of the proposed model, effects of overlay thickness, service temperature, fiber reinforcement, and tensile strength on the crack resistance of asphalt concrete overlays were observed. Figure 9 shows the theoretical predictions on the effect of temperature differential on the crack resistance of asphalt concrete overlays of various thicknesses at 0°C service temperature. The X-axis represents the joint opening displacement underneath the concrete slabs and the Y-axis represents the magnitude of the temperature differentials. Each data point represents a unit element length of crack advancement in the overlay. In the present case, each increment is 1/24 the depth of the overlay. The peak point associated with each curve in Figure 9 is also the point at which the crack extends from the interface to the top of the overlay (90 percent of the overlay thickness in the present study). The CMOD value at the joint-overlay interface is smaller than the critical crack opening displacement (which is about 0.102 cm for plain asphalt concrete and 0.178 cm for fiber-reinforced asphalt concrete at 0°C). This difference indicates that although the cohesive crack has propagated to the top of the asphalt concrete overlay, the bridging force along the crack surface is still there and a higher opening displacement (or more temperature differential) is needed to create a traction-free crack. Study of the effect of postcohesive process on the temperature crack resistance is still under way. For the present paper, the temperature differential resistance is defined as the peak temperature differential when the cohesive crack reaches the top of the overlay.

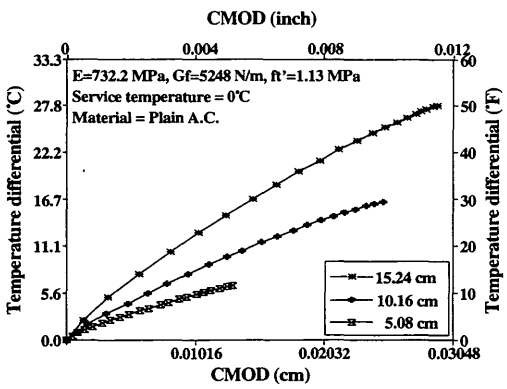

FIGURE 9 Effect of thickness on the crack resistance of plain asphalt concrete overlay at low service temperature (0°C).

Effect of Overlay Thickness

Figure 9 indicates that the thicker the overlays, the better the crack resistance to temperature differentials. This theoretical result also indicates that for the crack to propagate to the top in a thicker overlay, a larger joint contraction displacement (or CMOD), and thus a higher temperature differential, is

needed. This prediction is in agreement with field experience on the formation of reflective cracking; that is, increase of overlay thickness can retard the formation of reflective cracks in asphalt concrete overlays. A similar thickness effect is also predicted for higher service temperatures (i.e., 23°C), as indicated in Figure 10.

Effect of Service Temperature

As discussed earlier, the material properties (i.e., fracture energy, tensile strength, and Young's modulus; see Table 2) of asphalt concrete are highly temperature dependent. At different service temperatures, the material properties of the same mix can be very different. In general, the lower the service temperature, the higher the fracture energy, tensile strength, and resilient modulus. From Figures 9 and 10, it can be concluded that because of higher tensile strength and fracture energy, asphalt concrete overlays have better crack resistance to a temperature differential at a lower service temperature. In the meantime, at a lower service temperature, the magnitude of temperature differential and the contraction displacement of concrete slabs in the pavement also are much higher than those at normal service temperature. As a result, the improvement caused by a temperature-induced material property change may not be enough to compensate for the adverse effects caused by the drop in service temperature.

Effect of Fiber Reinforcement

The addition of fibers to asphaltic mixes in general increases the fracture energy by 50 to 100 percent, which implies that the fiberized mix is tougher and more ductile. Fiber addition, however, does not seem to have a significant effect on the material's modulus of elasticity or its tensile strength (see Table 2). Material properties of plain asphalt concrete (Series A) and fiberized asphalt concrete mixes (Series F and G) (*9*) were used to investigate the effect of fiber reinforcement. The peak temperature differentials of these three materials for various overlay thicknesses at service temperatures of 0°C and 23°C were reported in Figures 11 and 12, respectively. The

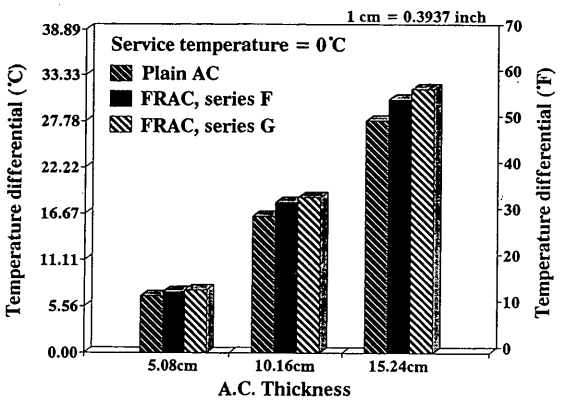

FIGURE 11 Peak temperature differentials of plain and fiberized asphalt concrete overlays at low service temperature (0°C).

fiberized asphalt concrete mixes have slightly better temperature crack resistance than does the plain asphalt concrete. This increase, however, is not very significant. However, because of the larger fracture energy values associated with the fiberized mix, it is expected that a much larger opening displacement is needed to generate a traction-free crack, which may add to the overall durability of the fiberized mix.

Effect of Tensile Strength

The effects of tensile strength on the reflective crack resistance were also analyzed with the other material properties (i.e., fracture energy and Young's modulus) being kept constant. Figures 13 and 14 show the effects of tensile strength on the crack resistance to temperature differentials for overlays of various thicknesses. The theoretical analysis indicates that the higher the tensile strength, the better the crack resistance to temperature differentials. The improvement is almost proportionate to the increase of the tensile strength.

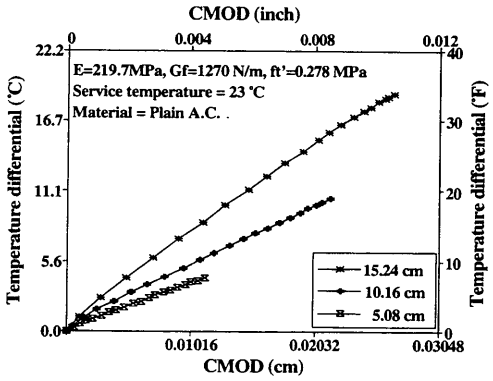

FIGURE 10 Effect of thickness on the crack resistance of plain asphalt concrete overlay at regular service temperature (23°C).

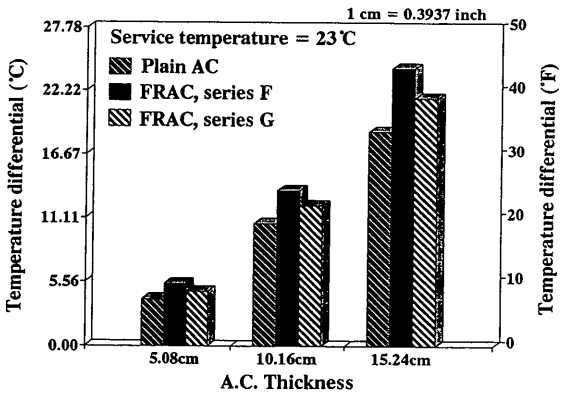

FIGURE 12 Peak temperature differentials of plain and fiberized asphalt concrete overlays at regular service temperature (23°C).

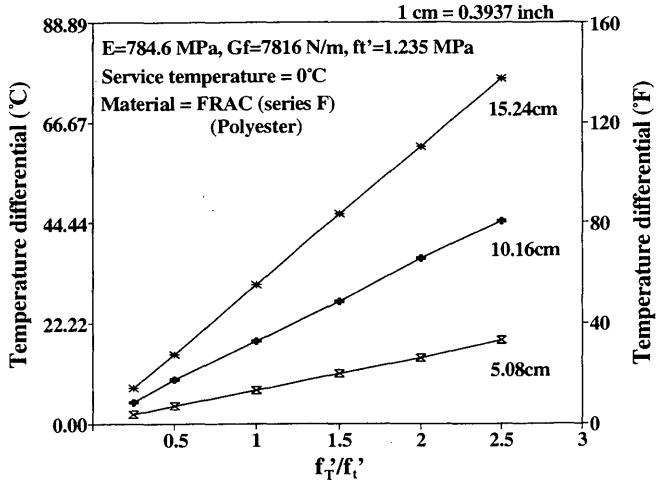

FIGURE 13 Effects of tensile strength on crack resistance of polyester-fiberized asphalt overlay at low service temperature (0°C).

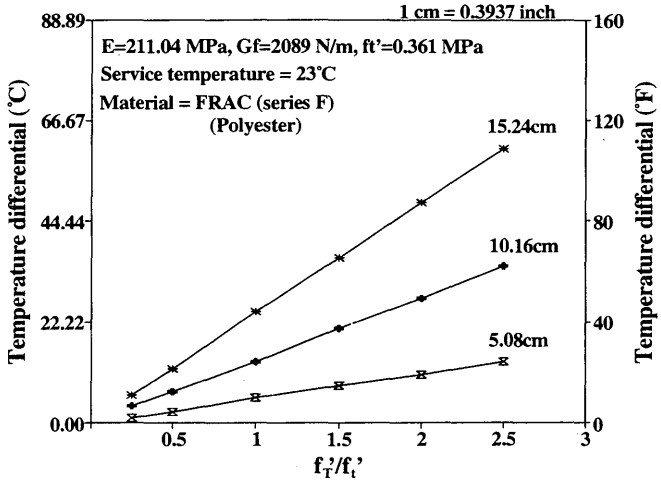

FIGURE 14 Effects of tensile strength on crack resistance of polyester-fiberized asphalt overlay at regular service temperature (23°C).

CONCLUSIONS

The following conclusions can be derived from the present study:

1. When temperature effect is the only consideration, the temperature crack resistance will be higher if a thicker asphalt concrete overlay is applied.
2. Crack resistance to the temperature differential at a lower service temperature was found to be better than that at a higher service temperature. However, this increase is not enough to prevent the frequently observed low temperature cracking in asphalt concrete caused by larger temperature differentials encountered at a much lower service temperature.
3. Temperature crack resistance of asphalt concrete overlays can be increased if the tensile strength of the asphaltic concrete mix is improved.
4. The proposed model provides a feasible approach to quantifying the crack resistance in asphalt concrete pavement systems. There is, however, a need for more research efforts to include effects, such as applied traffic loads, in the analysis.

ACKNOWLEDGMENTS

The authors appreciate the financial support provided by the Ohio Department of Transportation for the present research.

REFERENCES

1. D. S. Dugdale. Yielding of Steel Sheets Containing Slits. *Journal of the Mechanics and Physics of Solids*, Vol. 8, 1960, pp. 100–108.
2. G. I. Barenblatt. The Mathematical Theory of Equilibrium of Crack in Brittle Fracture. *Advances in Applied Mechanics*, Vol. 7, 1962, pp. 55–129.
3. A. Hillerborg, M. Modeer, and P. E. Petersson. Analysis of Crack Formation and Crack Growth in Concrete by Means of Fracture Mechanics and Finite Elements. *Cement and Concrete Research 6*, 1976, pp. 773–782.
4. Y. S. Jenq and J. D. Perng. Analysis of Crack Propagation in Asphalt Concrete Using A Cohesive Crack Model. In *Transportation Research Record 1317*, TRB, National Research Council, Washington, D.C., 1991, pp. 90–99.
5. J. D. Perng. *Analysis of Crack Propagation in Asphalt Concrete Using a Cohesive Crack Model*. M.S. thesis, The Ohio State University, June 1989.
6. S. H. Carpenter and R. L. Lytton. Procedure for Predicting Occurrence and Spacing of Thermal-Susceptibility Cracking in Flexible Pavements. In *Transportation Research Record 671*, TRB, National Research Council, Washington, D.C., 1978, pp. 39–46.
7. J. M. Armaghani, T. J. Larsen, and L. L. Smith. Temperature Response of Concrete Pavements. In *Transportation Research Record 1121*, TRB, National Research Council, Washington, D.C., 1987, pp. 23–33.
8. J. M. Richardson and J. M. Armaghani. Stress Caused by Temperature Gradient in Portland Cement Concrete Pavements. In *Transportation Research Record 1121*, TRB, National Research Council, Washington, D.C., 1987, pp. 7–13.
9. Y. S. Jenq and P. Liu. Effects of Fiber Reinforcement on the Crack Resistance of Asphalt Concrete. Presented at 71st Annual Meeting of the Transportation Research Board, Washington, D.C., Jan. 12–16, 1992.

Publication of this paper sponsored by Committee on Pavement Rehabilitation.